Directional frequency and recording (DIFAR) sensors in seafloor recorders to locate calling bowhead whales during their fall migration[a)]

Charles R. Greene, Jr.,[b)] Miles Wm. McLennan, and Robert G. Norman
Greeneridge Sciences, Inc., 1411 Firestone Road, Goleta, California 93117

Trent L. McDonald
Western EcoSystems Technology, Inc., 2003 Central Ave., Cheyenne, Wyoming 82001

Ray S. Jakubczak
BP Exploration (Alaska) Inc., 900 East Benson Boulevard, Anchorage, Alaska 99519-6612

W. John Richardson
LGL Ltd., environmental research associates, 22 Fisher Street, POB 280, King City, Ontario L7B 1A6, Canada

(Received 7 November 2003; revised 1 May 2004; accepted 3 May 2004)

Bowhead whales, *Balaena mysticetus*, migrate west during fall ~10–75 km off the north coast of Alaska, passing the petroleum developments around Prudhoe Bay. Oil production operations on an artificial island 5 km offshore create sounds heard by some whales. As part of an effort to assess whether migrating whales deflect farther offshore at times with high industrial noise, an acoustical approach was selected for localizing calling whales. The technique incorporated DIFAR (directional frequency and recording) sonobuoy techniques. An array of 11 DASARs (directional autonomous seafloor acoustic recorders) was built and installed with unit-to-unit separation of 5 km. When two or more DASARs detected the same call, the whale location was determined from the bearing intersections. This article describes the acoustic methods used to determine the locations of the calling bowhead whales and shows the types and precision of the data acquired. Calibration transmissions at GPS-measured times and locations provided measures of the individual DASAR clock drift and directional orientation. The standard error of the bearing measurements at distances of 3–4 km was ~1.35° after corrections for gain imbalance in the two directional sensors. During 23 days in 2002, 10 587 bowhead calls were detected and 8383 were localized. [DOI: 10.1121/1.1765191]

PACS numbers: 43.30.Sf, 43.30.Yj, 43.80.Nd [WWA] Pages: 799–813

I. INTRODUCTION

Whales use sound to communicate and to acquire information about their environment. Also, they often react to man-made sounds by changing their behavior and swimming away, or occasionally toward, the sound source (Richardson *et al.*, 1995, 1999). Beginning in late August and continuing past mid-October, bowhead whales (*Balaena mysticetus*) migrate west across the Beaufort Sea, swimming parallel to the north coast of Alaska (Moore and Reeves, 1993). The majority of the whales travel along a corridor 5–40 n.mi. (10–75 km) offshore, with the southern part of that corridor being through water <25 m deep. Alaska Eskimos have traditionally hunted these whales for subsistence (Stoker and Krupnik, 1993). The whalers are concerned about any industrial activity that might result in the bowheads swimming farther offshore and therefore being more difficult to hunt and retrieve.

In early 2000, BP Exploration (Alaska), Inc., began constructing its Northstar oil development, the first oil production facility seaward of the barrier islands in the Beaufort Sea. The development is centered on Northstar Island, an artificial gravel island 5 km seaward of the coastal barrier islands (Fig. 1). Oil production and gas injection began in late 2001, powered by gas-turbine engines, and drilling of additional wells continued through 2002. Northstar is 27 km west of a natural island (Cross Island) from which migrating bowhead whales are hunted in fall. Thus, the possible effects of the industrial operations on the whales, and on their accessibility to subsistence hunters, were of concern.

Because of both BP corporate policy and regulatory requirements, BP decided to study any possible effects of island sound on the path of migrating bowheads. The primary question was whether the whales passing Northstar were farther offshore during times when more sound was emitted from the island and its associated vessels. The approach taken was based on use of a passive acoustic method to determine the locations of calling whales. An acoustical method was selected, in preference to aerial surveys, because acoustics works 24 hours/day, during good weather and bad, night and day, and allows simultaneous monitoring of a large

[a)]Portions of this work were presented at a workshop on acoustic detection and localization of marine mammals. The workshop sponsor was DRDC Atlantic, Dartmouth, Nova Scotia; the dates were 19–21 November 2003. An abstract is to appear in the *Canadian Journal of Acoustics*.

[b)]Electronic mail: cgreene@greeneridge.com

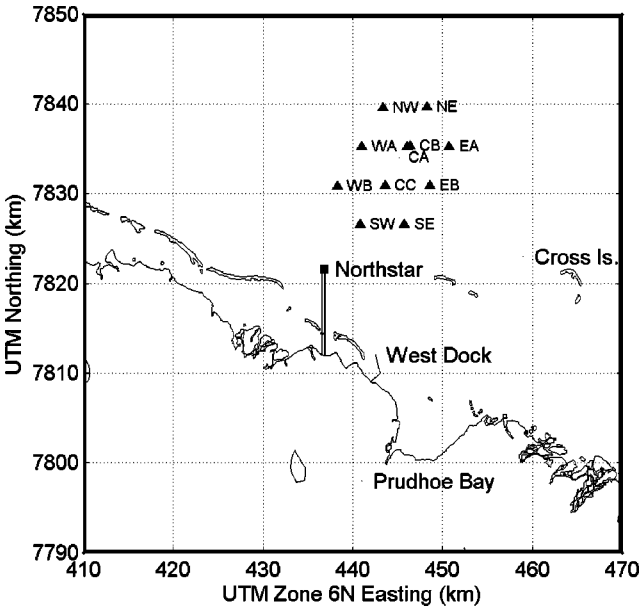

FIG. 1. Map of the central Alaskan North Slope including Prudhoe Bay and Northstar Island.

area. Previous experience showed that thousands of bowhead whale calls would be detected during one autumn season of monitoring, providing a far larger sample size than could be obtained from aerial surveys. To compare whale locations with sound emissions, continuous data on sounds from the island were needed. These were obtained with a hydrophone near the island, connected by cable to a digital recording system on the island. Statistical analyses were essential to assess whether any ''displacement'' effect was evident at times of high sound emission and, if so, to determine the magnitude of displacement. To date, field work has been done during the early autumn of 2000, 2001, and 2002, with equipment development and a pilot study in 2000, and effective data collection in 2001 and 2002. The study is continuing in 2003.

This paper describes the acoustical methodology developed to detect bowhead whale calls and to locate their source positions. Although the approach was the same in 2001 and 2002, some improvements were made from 2001 to 2002, and the following specific description concerns the 2002 techniques. Some results from 2002 are included to illustrate the approach and the nature and precision of the resulting data. Another paper (McDonald and Richardson, 2003) describes the statistical approach that has been developed for analysis of the whale locations versus sound emission data.

II. METHODS

There are two basic methods by which passive acoustic (hydrophone) data can be used to locate the sources of underwater sounds: hyperbolic fixing and triangulation (McLennan and Greene, 1996). Hyperbolic fixing involves measuring differences in the times when a given sound arrives at pairs of hydrophones, usually with cross-correlation. This method has been used extensively in previous studies of bowhead whales (e.g., Greene, 1987; Clark *et al.*, 1996). Triangulation involves measuring bearings to sound sources from two or more known locations, and then computing the intersections of the bearings.

Hyperbolic fixing with cross-correlation generally performs very well, but it requires synchronized timing of all the hydrophone signals. This is possible if the hydrophone signals are cabled or radioed to a common recording or processing point with a single clock. However, it is difficult to have precise timing with autonomous, asynchronous recorders, each with its own clock, as required here. Surface buoys were undesirable because of hazards from drifting ice, and interconnection by bottom cables was impractical.

Triangulation was chosen for this study because synchronized timing of autonomous units would be difficult to achieve, but autonomous bearing measurements could be obtained. Directional frequency and recording (DIFAR) sonobuoys (AN/SSQ-53) use a three-channel sensor from which azimuthal bearings to sound sources can be computed. Standard DIFAR sonobuoys have been used previously to obtain bearings to calling bowhead whales (Ljungblad, 1986; Greeneridge Sciences unpublished data) and to other baleen whales (e.g., Swartz *et al.* 2003). We incorporated DIFAR sensors from Sparton Electronics (De Leon Springs, FL) into seafloor recorders called DASARs, for directional autonomous seafloor acoustic recorders. A DASAR records the three DIFAR channels directly to disk in the seafloor recorder. An array of 11 DASARs deployed in the southern part of the whale migration corridor offshore of Northstar provided the needed intersecting bearings to the calling whales.

A. DIFAR principles

The concept of DIFAR is to use two horizontal, orthogonal directional sensors and an omnidirectional pressure sensor to sense an acoustic field. The directional sensors are particle velocity hydrophones with dipole patterns. A DIFAR sonobuoy uses a magnetic compass to provide a geographic reference. However, the DASARs (unlike drifting sonobuoys) sit firmly on the bottom and normally do not move after installation. Their locations are measured during installation with GPS. Thereafter, acoustic calibration transmissions from known locations around each DASAR can provide information on its reference direction with respect to grid north. As shown in Sec. III (later), this can provide more precise bearing data than could be obtained by reference to the compass built into a standard DIFAR sensor, especially during operation at high latitudes where magnetic compasses are less accurate and less stable.

Figure 2 shows the DIFAR sensor pattern. The orthogonal directional sensor patterns are circular, corresponding to a dipole response. A sound from a given direction results in received levels determined by the dipole response patterns. The angle to the source, relative to the reference axis, is determined from the arctangent of the ratio of the two response magnitudes. The phases of the dipole signals relative to the omnidirectional signal resolve the bearing ambiguities that would otherwise result from the arctangent.

The DIFAR sensor functions as if it were a three-channel analog device, including the following outputs:

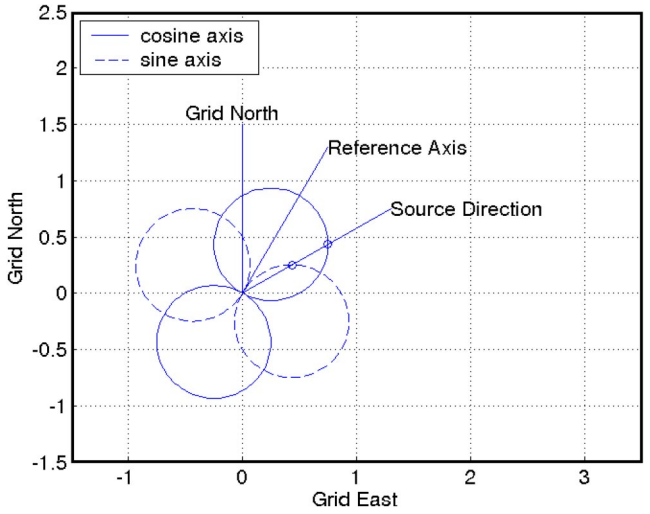

FIG. 2. DIFAR sensor omni and dipole patterns and reference angle. The angle between the reference axis and the source direction is the angle b used in the section on DIFAR principles.

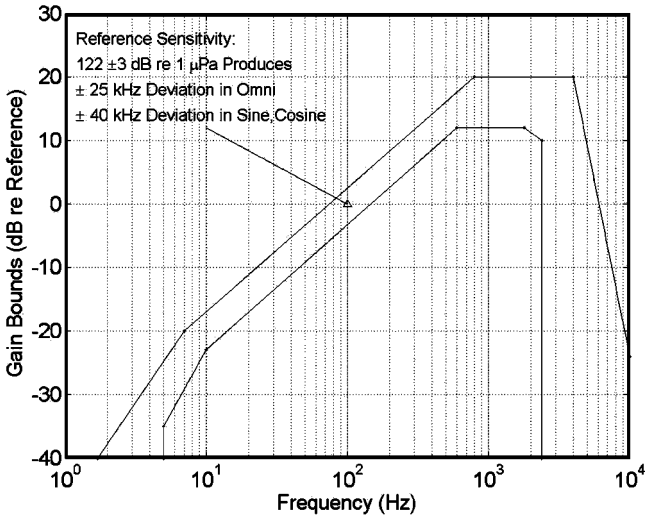

FIG. 3. DIFAR frequency response envelope. The response is specified to be within ±3 dB at 100 Hz.

(i) omnidirectional pressure sensitive hydrophone, and
(ii) two horizontal, orthogonal particle motion sensors whose outputs are proportional to the cosine and sine of the direction to the source. One is the ''cosine channel'' and the other is the ''sine channel.''

The DIFAR sensor reference axis is aligned with the cosine channel maximum (Fig. 2).

Assume the DIFAR sensor is mounted in the water away from any reflecting surfaces and interfering sound sources. Assume there is a source emitting sinusoidal waves so the instantaneous pressure at the omnidirectional sensor is

$$P_o(t) = A \sin(\omega t),$$

where A is the peak amplitude, ω is the radian frequency, and t is time. If the source direction is at bearing angle b from the reference axis, the instantaneous outputs of the cosine and sine channels will be

$$P_c(t) = \cos(b) \cdot A \sin(\omega t),$$

$$P_s(t) = \sin(b) \cdot A \sin(\omega t).$$

These two channels, plus the omnidirectional pressure channel, are recorded in the DASAR for offline processing. The direction can be found by forming the instantaneous products

$$Qoc(t) = Po(t) \cdot Pc(t) = \cos(b) \cdot A^2 \sin^2(\omega t),$$

$$Qos(t) = Po(t) \cdot Ps(t) = \sin(b) \cdot A^2 \sin^2(\omega t).$$

Taking the time average of the two products results in the bearing b in degrees as

$$b = 57.2957 \cdot \text{arctangent}(\text{mean}(Qos)/\text{mean}(Qoc)),$$

where the arctangent is defined for four quadrants.

If other sound sources are audible simultaneously, their signals add to the above expressions and distort the process. Thus it is important to exclude other sources as much as possible. In our processing of the DASAR data, the time and frequency extents of each whale call are first determined by inspection of a spectrogram. Then the signal is time-gated and bandpass filtered tightly before computing the products. These products are derived separately for every 1-ms time sample within the duration of a given bowhead call (typically 1–3 s), and then averaged across the call duration. The resulting averages are used to derive the estimated bearing to that whale call relative to the reference axis.

Alternatively, the bearing can be computed from the magnitude and phase of the discrete Fourier transforms of the three sensor channels. For a signal whose frequency changes or spans a range of frequencies, the bearings for every frequency component in the call can be computed and averaged to improve the bearing estimate. In our experience, the time domain and the frequency domain approaches yield very close to the same result. After initially deriving a bearing to each call via both approaches and finding little difference in the results, we now rely on the time-domain method. However, in Sec. III we present an example of the frequency-domain method.

The DIFAR specification for sonobuoy bearing accuracy calls for angles with respect to magnetic north to be within ±10°. Much better accuracy has been achieved with the DIFAR sensors incorporated into DASARs as described below, with the DASARs firmly on the bottom, calibrated externally, and not reliant on a magnetic compass (see Sec. III).

Figure 3 graphs the frequency response of DIFAR sonobuoys. It is specified to be from 10 to 2400 Hz, but there is some sensitivity at both higher and lower frequencies. The response is deliberately not flat; it rises with increasing frequency up to ~1000 Hz. This rise is to counter the natural drop in ocean ambient noise with increasing frequency, providing improved dynamic range and noise performance, especially at low frequencies. Most bowhead calls occur in the frequency range from 50 to 400–500 Hz (Clark and Johnson, 1984; Würsig and Clark, 1993), so the DIFAR coverage is an excellent match.

B. Directional autonomous seafloor acoustic recorder (DASAR)

The DASAR was conceived to incorporate DIFAR technology in an autonomous recorder that would operate for at

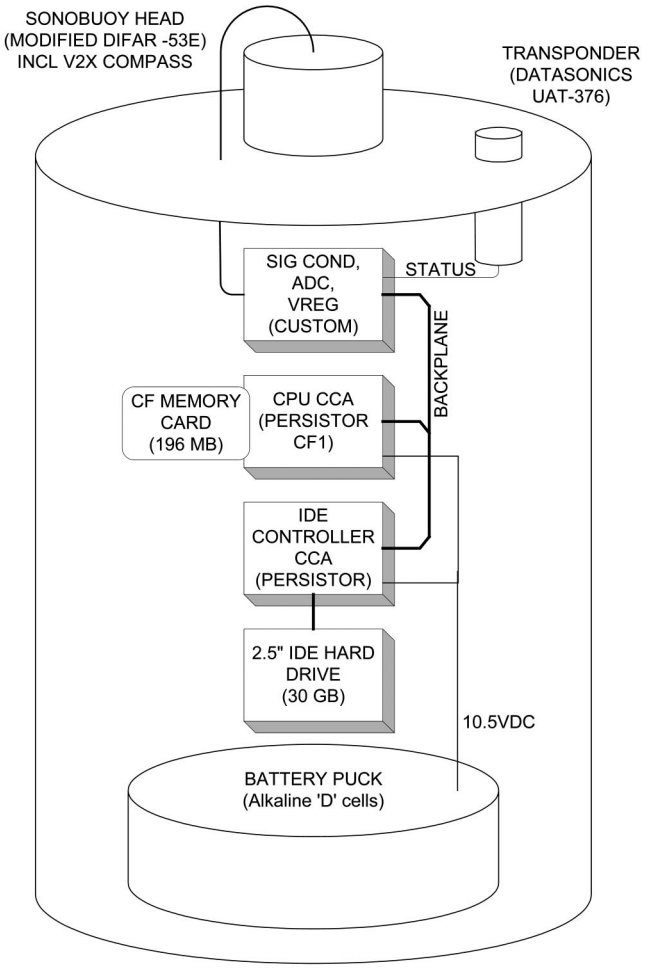

FIG. 4. Block diagram of the DASAR recording system.

least 30 days in the water north-northeast of Northstar Island, at depths up to 30 m. To achieve frequency coverage from 50 to almost 500 Hz, a sample frequency of 1000 samples/second was selected. For anti-aliasing, the three acoustic channels were lowpass filtered at 400 Hz. With three acoustic channels, 3000 samples/second had to be written to a computer disk storage unit.

Although DASAR orientation on the bottom was determined by calibration (see below), a compass was still desired in the DASAR as a check on any possible changes in orientation during a deployment. The compass in the standard DIFAR sensor used excessive battery power because of the high effective sample rate needed for the acoustic data. However, we did not require frequent compass readings. A substitute flux-gate compass, small in size and low in power drain (Model V2X from PNI Corp., Santa Rosa, CA), was installed in the sensor. Its output was recorded once for every disk write, which occurred at intervals of 46.6 min. Compass bearings were stored in the compact flash memory in the DASAR, independent of the disk storing the acoustic data.

1. Digital recording

Figure 4 is a block diagram of a DASAR. A Persistor Instruments Inc. (Bourne, MA) single-board computer, model CF1, serves as the central processor unit and controls the sampling, buffer storage, and disk recording from the buffer. The instrument uses a 196-MByte compact flash memory for double buffering so no data are lost during the disk write operation. However, in practice, the sounds of the disk drive increased the local acoustic noise for about 30 s each time disk writing occurred, once every 46.6 min. A disk of 30-GByte capacity (IBM Travelstar 2.5″) provides continuous storage for over 45 days' recording. The disk is controlled by Persistor Instruments' ''BigIdea'' IDE controller. A custom circuit card handles signal conditioning, analog-to-digital conversion for the three DIFAR channels, compass I/O, and various switching and linear regulators to power the CF1, compass, and sensor head.

2. Transponder for health checks

An acoustic transponder (Benthos model UAT-376, North Falmouth, MA) was built into each DASAR to permit checks on operational health during a deployment. This was essentially a check on the digital recording. If a sensor quit working, it was not likely to be reported as ''bad health.'' The transponder was powered by its own 9-V cells so it would continue operating if the main DASAR batteries failed. Upon interrogation at 26 kHz by a topside unit, each transponder transmitted on one of seven frequencies: 25, 27, 28, 29, 30, 31 or 32 kHz. In the DASAR application, the transponders were modified so that the frequency selection could be altered from the embedded controller. In this manner, one of two codes corresponding to ''OK'' or ''failed'' could be asserted.

The topside unit was a Benthos model DRI-267A, built as a diver-operated transponder/interrogator and deployed on a hand-held pole over the side of a boat. Upon receipt of transponder signals, it read out distance as well as the operational code. It operated over distances of at least 200 m, but GPS always brought the boat to within about 40 m of the DASAR being interrogated. In this project, the ''health'' of each deployed DASAR was checked about once per week. No failures were detected in 2002, but in 2001 some reports of ''bad health'' were received, and in these cases it was possible to retrieve and replace the failed DASAR.

3. Physical construction and batteries

The pressure housing is a cylinder 12 in. in diameter and 14 in. high (30×36 cm). The recording electronics and the transponder are mounted on the underside of the lid, which incorporates double O-ring seals. Three packs (Nexergy model SMP-7S4P, Escondido, CA) of 28 D-cell alkaline batteries are wired in series and parallel to provide 10.5 V. They are secured by a plate and threaded rods anchored in the cylinder bottom. Diodes protect the packs from internal shorts.

On the top of the DASAR are two plastic posts 8.75 in. (22 cm) tall, extending upward from opposite sides of the top plate. Between them is a rubber band 1 in. (2.5 cm) wide from which the DIFAR sensor is suspended. The top of the sensor is secured to a plastic block with a double O-ring seal. The wires from the compass and three acoustic sensors pass from the sensor through the block and into a plastic tube and

FIG. 5. DASAR on deck with anchor and tag line, ready for deployment. Also on deck are other DASARs without their protective socks.

thence to a waterproof access in the main body of the DASAR. The rubber suspension permits the sensor to ''float'' relatively freely in the water for sensing the particle motion essential to the directional sensing, while at the same time minimizing twisting.

As deployed in 2002, a latex ''sock'' secured over an aluminum cage shielded the sensor from motion induced by water currents. Figure 5 portrays a DASAR in its sock on the deck ready for deployment with the small anchor and tag line. (In 2001, a different frame and a self-supported thin plastic dome were used.) Each DASAR was installed on the bottom with a tag line between the DASAR and an anchor, both of whose positions were measured by GPS during deployment. No surface buoys were used because of hazards from drifting ice floes. The DASARs were retrieved from depths of 16–24 m by grappling for the tag line based on the GPS coordinates.

C. The DASAR array

The basic array configuration is a series of equilateral triangles. Bearing measurements from pairs of elements in a triangle provide good resolution of source location for sources at any angle around the triangle. Six triangles sharing a center unit formed a hexagon (Fig. 6). Two overlapping hexagons completed the array of ten locations oriented roughly north-northeast from Northstar Island, toward the path of migrating bowheads. The basic spacing between adjacent DASARs was 5 km (2.7 n.mi.), selected based on known bowhead call detection distances of 15–20 km and experience with 2-km spacing in a 1986 application of passive localization (Greene, 1987). The closest and farthest units were, respectively, 7 and 22 km (4 and 12 n.mi.) northeast of Northstar, with the most offshore unit being about $\frac{1}{3}$ of the distance from Northstar to the shelf-break.

Twelve DASARs were constructed and tested. Two were intended to be spares, but it made sense to deploy one of the spares as a redundant element at a central location in the ten-position array. Thus, two DASARs were used at the center of the northern hexagon, spaced about 200 m apart at locations CA and CB (Fig. 6).

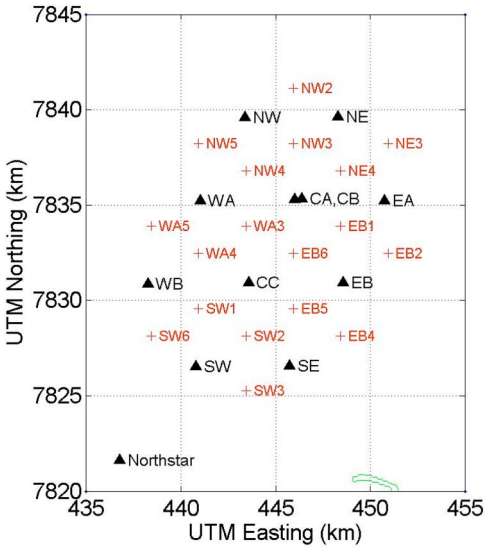

FIG. 6. Map of DASAR locations with respect to Northstar Island. The stations from which calibration signals were transmitted are also shown.

D. Time and reference axis calibration

Calibrations were very important to the success of the triangulation approach to whale call localization. The times had to be known within 1–2 s to permit associating calls received on two or more independent DASARs, as necessary to localize based on bearings from two or more DASARs to the same call. With 5 km between adjacent DASARs, the maximum difference in acoustic travel time to an adjacent pair of DASARs is 3.3 s. The travel time across the longest separation of DASARs (units NE and SW in Fig. 6) is 10 s.

Reference axis calibration was very important to minimizing localization errors. Clearly, the smaller the uncertainty in the bearing measurements, the smaller the uncertainty in the whale call location. A detailed description of localization errors is contained in Appendix B.

The approach taken to calibration for both time and reference axis direction was to transmit a signal from a boat at known locations around and within the DASAR array. The equipment included a U.S. Navy model J-9 underwater sound projector (U.S. Navy Sound Reference Laboratory, Newport, RI), a 400-W Mackie FR series M-800 amplifier (Woodinville, WA), a notebook computer, and a Trimble Lassen Model 39261-10 (Sunnyvale, CA) GPS receiver with a pulse time signal output precisely at every UTC (Universal Time Coordinated) second. The notebook computer contained the waveform file and reproduced it for amplification and transmission on receipt of the timing signal from the GPS. Although the J-9 is not rated for source levels greater than ~150 dB *re* 1 μPa·m, its efficiency is very low and a high-powered amplifier is required to achieve such a source level.

The waveform of the calibration signal required a clear start time for clock timing and wide bandwidth for determining the reference axis bearing. The sound waveform used in 2002 began with a 400-Hz tone for 5 s, followed by a 2-s gap, a downsweep from 400 to 200 Hz, another 2-s gap, an upsweep from 200 to 400 Hz, a 2-s gap, and a final downsweep from 400 to 200 Hz. (In future applications, the 2-s

TABLE I. DASAR calibration results for 2002, including corrections for gain imbalance in the two directional channels and clock drift coefficients.

DASAR location	Total Pings	Original ref. bearing (deg)	Corrected ref. bearing (deg)	Gain factor	Original std. dev. (deg)	Corrected std. dev. (deg)	Clock drift (s/day)	Scatter after fit (s)
NW	126	89.9	89.5	1.0607	1.50	0.87	−0.4836	0.19
CC	198	248.9	248.8	1.0270	1.70	1.60	−1.3582	0.16
WB	138	34.3	34.0	1.0286	1.30	1.20	−1.7558	0.22
CB	194	157.0	157.0	1.0883	2.30	1.50	−1.1756	0.28
CA	192	186.9	187.0	1.1337	2.60	0.99	0.3827	0.21
EA	139	58.6	57.6	1.1594	2.90	0.93	−1.1898	0.34
WA	165	192.9	192.3	0.8661	3.30	1.30	−1.3838	0.19
SE	127	26.7	26.7	1.0038	0.80	0.80	−1.9505	0.54
SW	33	59.0	59.5	1.0781	3.60	3.30	−0.2753	0.30
NE	135	96.0	95.7	0.9294	2.50	0.80	−1.1723	0.21
EB	154	190.5	190.8	1.0529	1.90	1.60	−0.7723	0.19
					Avg: 2.22	Avg: 1.35		

gaps will be omitted.) The total duration of one transmission was 22 s. For each calibration location, two full transmissions occurred at sound projector depth 9 m followed by two more at depth 6 m. All transmissions were analyzed as received at the closest two or three DASARs, generally within distance 3–4 km.

Calibration stations were selected in and around the array such that each DASAR received calibration signals from at least four (and often six) nearby stations on different bearings. Figure 6 shows the 18 calibration stations used in 2002 in relation to the 11 DASARs. Obtaining bearings to several known sites around each DASAR permitted searching for possible systematic bearing errors. One such error was found and attributed to ''gain imbalance'' between the two directional channels.

E. Gain imbalance between the directional sensors

The DIFAR sensor manufacturer, Sparton Electronics, employs careful calibration techniques to equalize the sensitivities of the sensors for the two directional channels. However, the manufacturing specification is for bearing accuracies of $\pm 10°$ and we desired better performance. There was evidence in our data that, as installed in the Beaufort Sea, the gains (sensitivities) of the DIFAR sensors were slightly unbalanced, resulting in systematic bearing errors. A gain-correction procedure has been developed. It is described in Appendix A.

F. Localization process and its accuracy

The locations of the calling whales were estimated based on triangulation. However, when more than two bearings to a given call were available, the 2+ intersections of bearings usually did not coincide exactly. A maximum-likelihood approach was developed to estimate the most likely location, taking account of the variability in bearings from each DASAR as determined during calibration. Also, an estimate of the precision of each whale call location was used as a weighting factor in subsequent statistical analyses (McDonald and Richardson, 2003). Appendix B describes the localization process and the derivation of the localization accuracy measures.

G. High background noise cutoff distance

The objective of the project was to evaluate whether offshore distances of whales were related to the level of industrial sound measured near the island (400 m away). Early data indicated that, during higher background noise conditions (>96 dB *re* 1 μPa broadband) at the DASAR array, fewer whale calls were detected. Further analysis confirmed that, at such times, proportionally fewer calls were detected at longer distances. To minimize the influence of variations in background noise on the observed distribution of whale call locations, it was necessary to limit the study area to the region within which whale calls were likely to be detected even during high noise conditions. The appropriate distance was determined by comparing the distribution of distances from the array-center to the detected whale calls during times with high and low background noise (see Sec. III).

III. RESULTS

Examples of the results of the calibration process and the localization of whale calls for 2002 are presented here. McDonald and Richardson (2003) show how these results can be analyzed statistically to assess whether bowhead whales are displaced offshore at times when much industrial sound emanates from the Northstar area. In 2002, the DASARs were deployed on 30–31 August and recovered on 3 October. One DASAR apparently physically tipped over on 4 September, but the other ten functioned well until 23 September when all apparently tipped over during an unusually strong storm. Thus, the effective study period was from 31 August to 23 September. Health checks were done about once per week, and there were no reports of ''bad health.'' (In 2001, some such reports were received, and this allowed us to replace failed units with functional ones.)

A. Calibration of DASAR clock times and reference axis bearings

The calibration results for each DASAR are presented in Table I. Calibration data were collected on 2, 7, 13 and 21 September 2002. For 10 of 11 DASARs, the calibration was based on 126–198 calibration pings. For the DASAR at location ''SW,'' only 33 pings (all from 2 September) were useable; SW was the unit that upset in high storm surge on 4 September.

The benefit of correcting for the gain imbalance between the two directional sensors of each DASAR is evident by comparing the standard deviations of the ''original'' (uncorrected) bearings, which averaged 2.22°, with those of the ''corrected'' bearings (average 1.35°). Corresponding average values for 2001 were, respectively, 6.60° and 6.28°. The higher values in 2001 resulted primarily from using tones as calibration sounds, in contrast to the frequency sweeps used in 2002. The year-to-year differences in the DASAR housings may have been a minor factor.

Based on the DIFAR sonobuoy specification that bearing errors should be within ±10°, standard deviations on the order of 3° had been expected. The improvement over the specification (in 2002) is partly from the broadband calibration signals used, partly from the gain-correction procedure, and partly because the orientations of the bottom-mounted DASARs were fixed and externally calibrated. In contrast, a DIFAR sonobuoy is designed to drift, with bearings being determined in relation to an internal magnetic compass.

The time-drift calibrations showed that the clocks in the DASARs drifted by as much as 2 s per day (Table I). However, the drift-rate was quite stable over time, a result expected given the frequency/temperature sensitivity of the crystal oscillator time base and the fact that the ambient temperature varies only slightly once deployed. After compensation for the measured drift, the times of events recorded between calibrations generally could be determined to an accuracy of 1 or 2 s. This was adequate for assessing whether a whale call received at several DASARs represented a single call from one whale. The residual measurement scatter is mostly due to imprecision in determining the time of the received signal during data analysis. This precision can be improved, as described in Sec. IV.

B. Whale call localization

During the period from mid-day on 31 August until mid-day on 23 September 2002, 10 587 whale calls were detected. Of these, 2022 (19%) were detected by only one DASAR and thus could not be localized. Also, 182 (2%) of the remaining 8565 calls did not yield a location because the maximum likelihood procedure (Appendix B) did not converge, and 461 (5%) of the remaining 8383 calls yielded a location but the variance-covariance matrix of the solution was not positive definite. Overall, 7922 (75%) of the 10 587 calls yielded useable locations in 2002.

Figure 7 presents an example of a whale call bearing measurement, in this case from DASAR unit EB. The bearings of all the 1-ms time samples spanning the duration of the call are plotted as vectors from the DASAR location. The

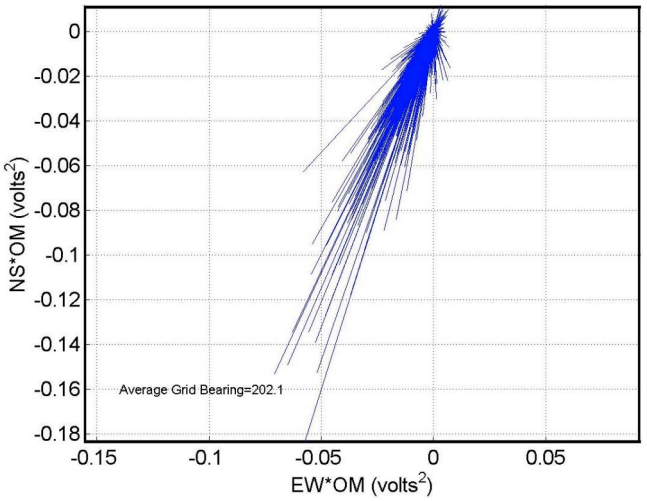

FIG. 7. Example of a time-domain bearing display illustrating the spread of the bearings computed for each 1-ms time sample. From the DASAR at location EB in 2002.

bearing estimate comes from the arctangent of the average of the north-south components divided by the average of the east-west components.

The same call as received at the same DASAR was also processed by the frequency domain method. Figure 8 presents the magnitude of the sound pressure density spectrum computed over the duration of the call as delimited by the analyst. The relatively high spectrum levels at 190–320 Hz represent the whale call. Figure 9 presents the bearing-frequency result for the same call, with the bearing selected from the time-domain solution superimposed across the frequencies selected by the analyst.

The specific call illustrated above was detected via six DASARs, and Fig. 10 shows the intersections of those bearings, including the bearing from Fig. 10 (unit EB). Of the 7922 useable call locations during the 23-day study period in 2002, the numbers based on 2, 3, 4, and 5+ bearings were 2085, 1429, 1129, and 3279, respectively.

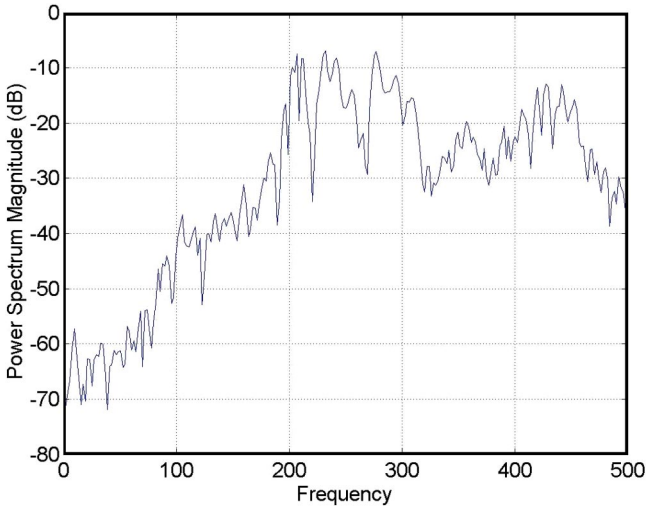

FIG. 8. Sound pressure spectral density for the whale call in Fig. 7. The peak at about 200–320 Hz represents the whale call. The increasing slope in the background noise is a result of the sloped sensitivity of the DIFAR sensor as shown in Fig. 3.

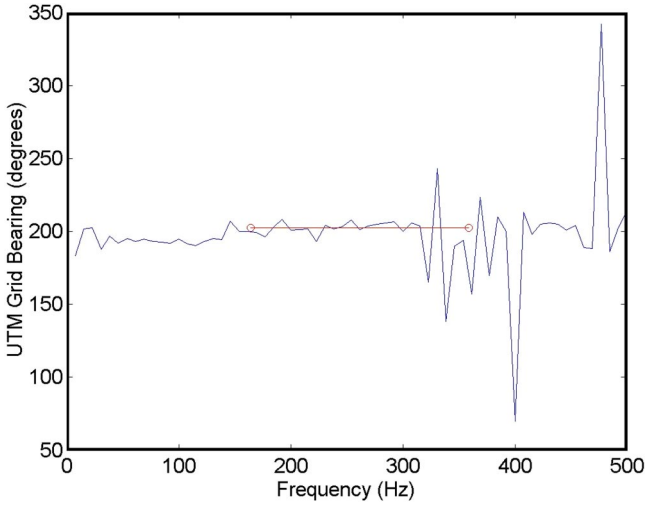

FIG. 9. The directional spectrum for the whale call in Figs. 7 and 8. The bearing from the time domain analysis (Fig. 7) is drawn for the frequency band selected by the analyst.

The numbers of bowhead whale calls detected per hour varied widely through the operational period (Fig. 11). Call detection rates depended not only on the number of whale calls, but also on the background noise level. High background noise (>90th percentile, 101 dB *re* 1 μPa broadband) tended to mask the more distant calls (see below). The best estimates of the locations of the 350 localizable bowhead whale calls detected on 14 September 2002 are mapped in Fig. 12.

C. Localization accuracy

Figure 13 maps one measure of the accuracy of whale call localizations for locations around the DASAR array, based on all 7922 of the useable call locations from 2002. The calculations were based on the estimated accuracy of individual locations, which in part depended upon error in the calibration bearings (see Appendix B). As expected, accuracy tended to deteriorate with increasing distance from the center of the array of DASARs. For most locations within the perimeter of the array, the length of the major axis of the 90% confidence ellipse based on asymptotic intervals averaged between 0.25 and 1 km. For most locations 10 km

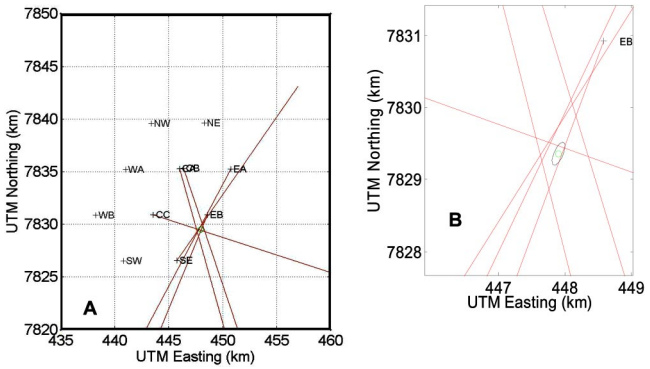

FIG. 10. Map of an example of intersecting bearings to a whale call. The bearing is included from unit EB for the call shown in Figs. 7–9. (a) Large area view. (b) Exploded view of the intersection area showing the 90% confidence ellipse and best estimate of calling whale's location.

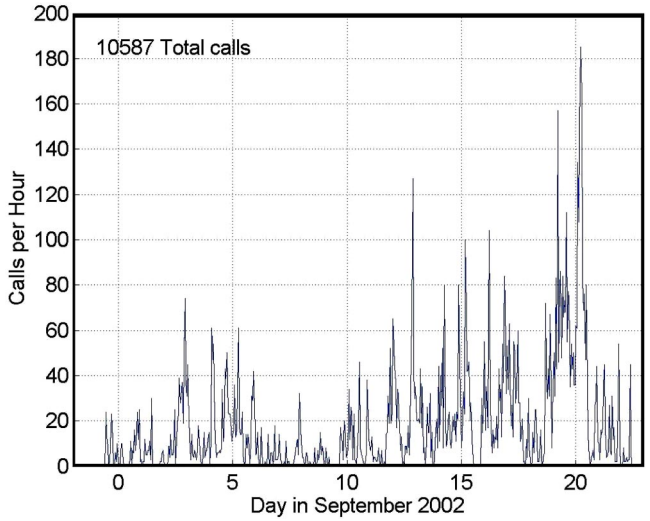

FIG. 11. Numbers of bowhead whale calls detected per hour over the period 31 August–23 September 2002. A total of 10 587 calls were received at one or more of the DASARs.

from the center of the array (~6 km outside the perimeter), the corresponding average was ~1 km. Average localization accuracy was apparently poorer in an area southwest of the DASARs (and northwest of Northstar), but very few calling whales were detected there. Beyond about 10 km from the center of the array, localization accuracy deteriorated rapidly (Fig. 13).

D. High background noise cutoff distance

Distances were determined from "center" DASAR CB to all whale calls detected during times of very high (>90th

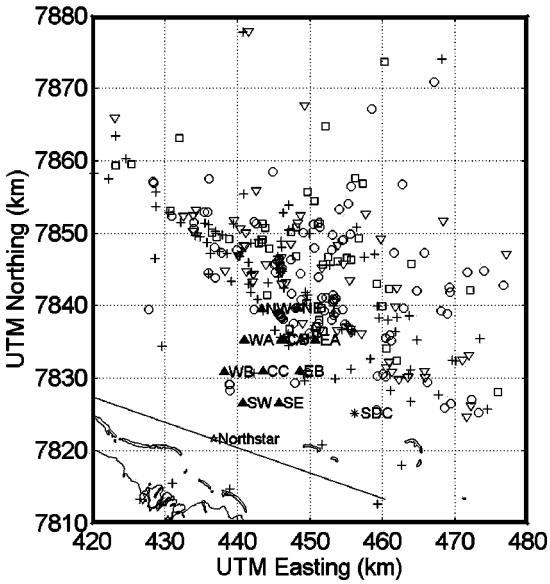

FIG. 12. Whale call localizations for 14 September 2002. Filled upright triangles represent DASAR locations. Symbol types discriminate calls whose locations were estimated based on bearings from two (+), three (▽), four (□), or more (○) DASARs. On this date, 42 calls (not localizable) were detected on only one DASAR, 115 calls on two DASARs, 65 with three DASARs, 55 with four DASARs, and 115 with five or more DASARs. The WNW-ESE line through Northstar Island shows the general trend of the coastline; the autumn bowhead migration is to the WNW, parallel to shore.

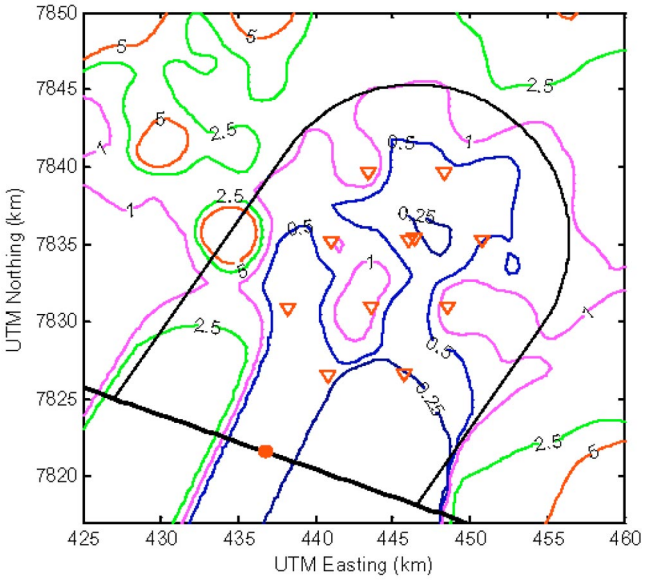

FIG. 13. Mean length (in meters) of major axis of 90% confidence ellipses around estimated call locations shown as a contour plot. Filled circle represents Northstar Island, open triangles represent DASARs, and the solid black line through Northstar is parallel to the (idealized) coastline. The horseshoe pattern oriented northeastward represents the area within which bowhead calls were retained for the displacement study.

percentile, 101 dB *re* 1 μPa broadband), moderately high (>75th percentile, 96 dB), and low (<25th percentile, 87 dB background noise) (Fig. 14). Background noise was measured at the DASAR farthest from Northstar (DASAR NE). The proportion of the detected calls that were at distances >10 km was lower during the very high and moderately high background noise conditions. To minimize potential biases, calls >10 km from the ''central axis'' of the DASAR array were not used in statistical analyses of call locations relative to Northstar noise. That central axis extended from CB to Northstar. Thus, the study area for those statistical analyses was a ''silo-shaped'' area (Fig. 13) that was 20 km wide extending offshore to DASAR CB, capped by a semi-circle of radius 10 km centered at CB.

IV. DISCUSSION AND CONCLUSIONS

Background noise has a strong influence on the detectability of whale calls. At times with high background noise (>101 dB *re* 1 μPa broadband), calls with low source levels, and other calls whose received levels at the DASARs are low because of propagation from long distances, are less likely to be detected. [See Blackwell and Greene (2004) for data on sounds, noise, and propagation at Northstar.] The variability in background noise is one reason why simple counts of whale calls (e.g., calls detected per hour) are not a reliable index of the number of whales in the area. (The potentially variable calling rate of individual whales is another reason.) In using the data from this project, it has been important to limit the size of the study area to a region where calling bowhead whales are generally detectable even when the background noise is high. In 2002, the ''high background

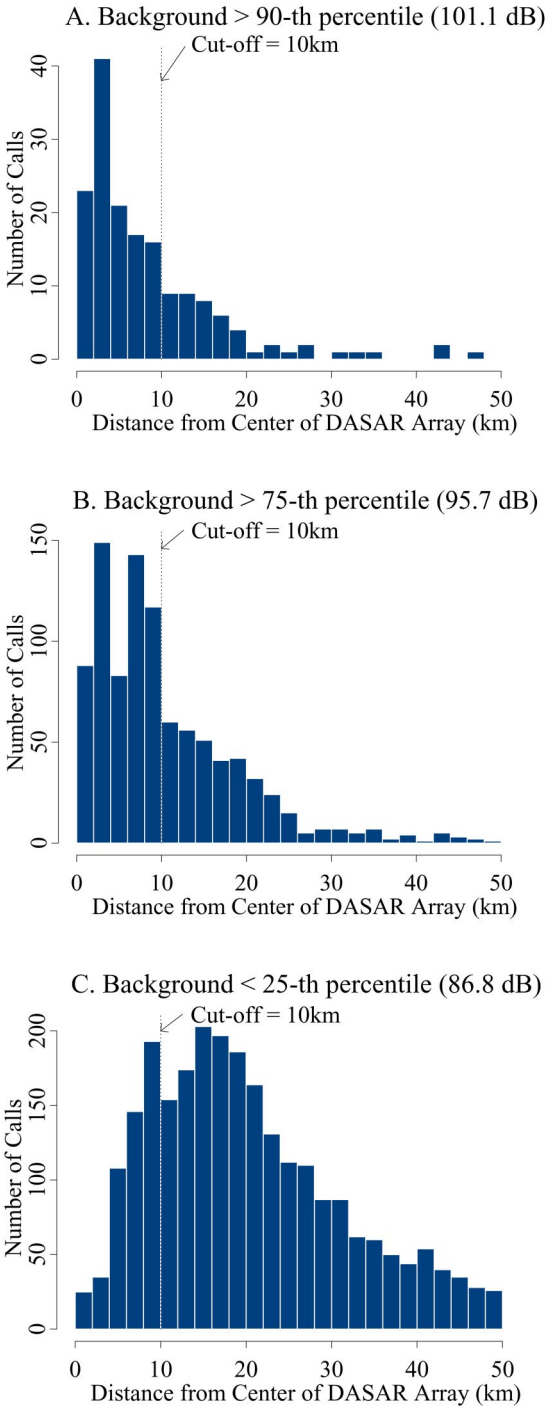

FIG. 14. Histograms of distance from estimated locations of calling whales to the center DASAR (CB) during very high (a), moderately high (b), and low (c) background sound conditions in 2002. A cutoff distance of 10 km was established at the ''shoulder'' evident in (a) and (b). Background sound was measured at the NE DASAR in the 5–500-Hz band.

cutoff distance'' was determined to be 10 km (Fig. 14). A corresponding analysis for 2001 showed it to be 12 km in that year (Greene *et al.*, 2002).

A. Comparison with hyperbolic localization

A well-known and widely used technique for passive acoustic localization is hyperbolic fixing based on arrival time differences at widely spaced sound pressure sensors. (A symposium on this method, as applied to the localization of

calling marine mammals, was held at Halifax in November 2003. The papers are to be published in the *Canadian Journal of Acoustics* during summer 2004.) The technique requires an accurate time base (~1 ms for sounds like bowhead whale calls) and involves crosscorrelating sensor pairs. Clark and Ellison (2000) reported a calibration experiment conducted during spring at Barrow, Alaska, to verify the accuracy of their analysis of bowhead call locations as determined via arrival-time differences. Their three sensors were roughly in line, spaced 670 and 946 m apart. Two theodolites spaced 482 m apart provided ''ground truth.'' Their acoustic bearing errors for angles not far from the normal to their baseline were on the order of 0.1° compared to about 1° for our DIFAR bearings at all azimuths. Multipaths frequently create significant uncertainties and biases in hyperbolic fixes, but propagation in the Barrow environment during spring was reported to be basically plane waves without reflections.

B. Potential improvements to DASAR performance

The controlling software will be revised to permit entering a sleep mode after initialization, with startup programmed for a time after the units are on the bottom and stable. In the past, when DASARs have been writing to disk while being handled, write failures have sometimes occurred.

In future applications, the sound transmitted for calibration of times and reference bearings will be frequency sweeps or a pseudo random noise waveform of at least 200-Hz bandwidth. Wideband sounds have been shown to produce less bearing scatter than tones. There will be no gaps in the sound transmissions. Also, 14 more calibration stations will be added to the 18 used in 2002 (Fig. 6), providing better azimuthal calibration data for the peripheral DASARs and hence better gain imbalance corrections.

Data analysis will be enhanced to permit more accurate measurements of the arrival times of the calibration transmissions. Also, more automation in detecting whale calls will be investigated. At present, whale calls are detected based on simultaneous visual inspection of spectrograms of the data from all active DASARs, one minute at a time. The computer might be programmed to detect whale calls by using their frequency characteristics and the fact that they are stronger than the background sounds (Mellinger and Clark, 1997, 2000).

C. Utility of DASARs in localizing sound sources

This application of DIFAR techniques, as incorporated into autonomous bottom-mounted recording units, has been successful in monitoring the locations of calling bowhead whales over extended periods in a remote region. This approach allows distributed data acquisition and requires only moderately accurate synchronization (e.g., ± 1 or 2 s) of the time bases of the various recording units. This approach is suitable in situations where it would be difficult or impossible to acquire all the data with a single recording system and time base, as needed for localization by time-of-arrival methods.

Experience from two years' use of DASARs to localize bowhead whale calls reinforces the concept of applying DIFAR sensor technology to sound source localization. The frequency range of 10–500 Hz, as presently recorded by the DASARs, suits the frequency ranges of most bowhead calls, and may also be suitable for most other baleen whales (Richardson *et al.*, 1995). However, the DIFAR sensors are useful at frequencies >2 kHz and could conceivably be used to detect and localize clicks from sperm whales and some other marine species. A higher frequency range would require a higher sampling rate, which would affect recording life depending on disk space.

The present DASAR units are designed for deployment in relatively shallow water and retrieval by a simple grappling technique. The physical configuration of the units would need to be revised if deeper deployments were required. However, the DIFAR-based approach should be useable in deeper water.

ACKNOWLEDGMENTS

Dave Iddings, Quy Nguyen, Bob Early, and Patrick Dexter designed the DASAR pressure housing, sensor suspension, and sensor wire routing (including waterproofing). Mark Cavalier, Nautronix-MariPro, fabricated the aluminum frames and cages. Kent Reinhardt of Sparton Electronics was very helpful with engineering details of the DIFAR sensors, permitting us to disable the built-in compass and extract the sensor signals before they were multiplexed. David Christian made the cable harness from the sensor to the recording electronics, and he wired the DASAR electronics and batteries, making battery installation simple and foolproof. During deployment, calibrations, and retrieval, crews of Alaska Clean Seas provided excellent navigation and seamanship consistent with safe operations. Jonah Leavitt of Barrow, Alaska, helped with mobilization at Deadhorse, Alaska, as well as deployment and retrieval at sea. Mike Williams of LGL helped in innumerable ways. Wilson Cullor and Allison Erickson of OASIS Environmental, on behalf of BP, helped with logistics planning for the fieldwork. Dr. Bill Streever of BP and Dave Trudgen of OASIS, also on behalf of BP, guided the project. BP Exploration (Alaska) Inc. supported the work. Two anonymous reviewers made helpful remarks. We thank them all.

APPENDIX A: GAIN IMBALANCE BETWEEN DIRECTIONAL SENSORS AND ITS EFFECT ON BEARING ACCURACY

Summary: This Appendix investigates gain imbalance between the two DIFAR directional sensors. A method is developed to quantify and correct for this factor, thereby improving the accuracy of measured bearings to whale calls. Calibration ping data taken for time and bearing calibration are analyzed to determine the imbalance.

1. Introduction

DIFAR hydrophones are the acoustic sensors in the DASARs. These small units were installed in water 20–25 m deep with an unknown orientation. To measure the orientation on the bottom and calibrate the clock time drift, acoustic pings were transmitted in the water from known locations.

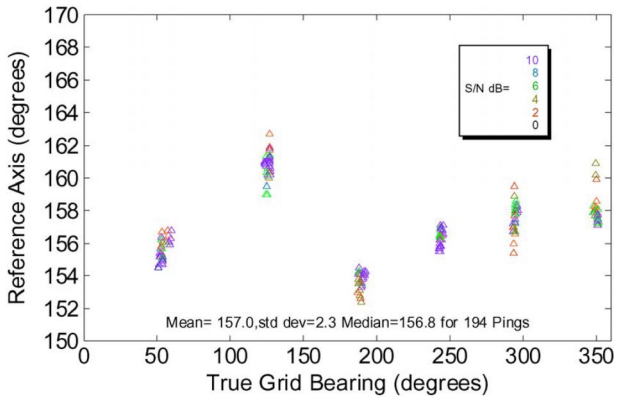

FIG. 15. Measured reference axis direction versus true grid bearing for DASAR CBa. From each location of the ping projector, 4–8 pings were transmitted. For each DASAR, bearings were determined to the pings projected from 4–6 positions at different azimuths. The vertical axis is the calculated bearing of the reference axis of the DIFAR hydrophone.

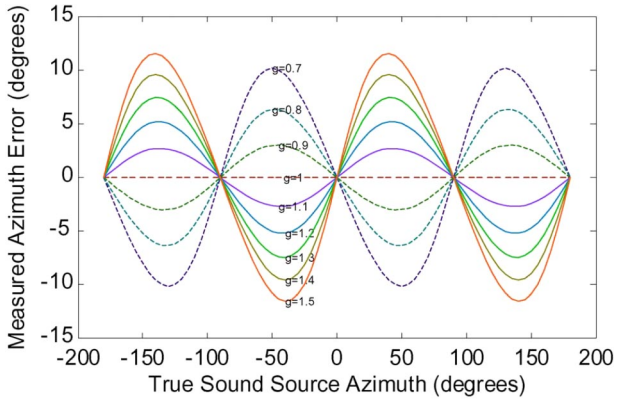

FIG. 16. Azimuthal bearing error due to DIFAR gain imbalance.

By measuring the bearing of each ping with the DIFAR logic and comparing it to the known bearing from the DASAR to the projector position, it was possible to measure the reference axis direction on the bottom.

The reference axis direction is given by

$$b_{\text{ref}} = b_{\text{true}} - b_d\,, \tag{A1}$$

where b_{true} is the known true bearing of the ping, and b_d is the measured DIFAR bearing relative to the reference axis direction.

Figure 15 presents the measured reference bearing for DASAR CB data plotted versus true bearing. The overall scatter is ~10° peak-to-peak. This meets the bearing accuracy specified for DIFAR, but is larger than desired. At any given true bearing, the scatter is on the order of 3°–5°, but the variation across bearing appears to follow an orderly pattern, suggesting that improvement would be possible if the cause of the variation could be determined and modeled.

Reflecting objects near the DASAR could explain some bearing error; however, the installation area is uniform and relatively flat. Vertical multipaths (which do exist) would not introduce azimuthal bearing errors. We were led to investigate the effects of a gain imbalance in the DIFAR directional channels and to find a means of correcting for it.

2. The effects of a gain imbalance

The DIFAR sensor includes three acoustic channels, one omni and two directional. The bearing measurement process requires that the acoustic sensitivity of the two directional channels be equal. The DIFAR sensor is complex and includes many adjustments by the manufacturer to match the outputs, including temperature compensation. However, the manufacturing specification permits bearing errors of ±10° and it appeared better performance was possible. Gain imbalance seemed a possibility. We first investigate what the effect would be of such a gain imbalance.

We introduce three new variables:

g gain factor of sine channel relative to cosine channel ($g=1$ means no imbalance)

b_{err} error angle introduced by the gain imbalance

b_{meas} measured bearing including the error, such that

$$b_{\text{meas}} = b_d + b_{\text{err}} \tag{A2}$$

Assume there is an acoustic signal of amplitude A arriving from bearing b_d relative to the DIFAR reference axis. The x and y components of that signal will be

$$\begin{aligned} vx &= A \sin b_d\,, \\ vy &= A \cos b_d\,. \end{aligned} \tag{A3}$$

However, if there is a relative gain error g, these will be measured as

$$\begin{aligned} vx_{\text{meas}} &= g \cdot A \sin b_d\,, \\ vy_{\text{meas}} &= A \cos b_d\,, \end{aligned} \tag{A4}$$

and the measured bearing will be

$$b_{\text{meas}} = \arctan(vx_{\text{meas}}/vy_{\text{meas}}) = \arctan(g \cdot vx/vy), \tag{A5}$$

where arctan is the form of the arctangent that accounts for all four quadrants. This measured bearing can be converted to the error b_{err} by subtracting the known b_d. Figure 16 shows the bearing error resulting from values of g ranging from 0.7 to 1.5.

When the error is plotted versus the true azimuth, it very closely resembles a sine wave with two cycles in the 360° of azimuth, with amplitudes ranging up to about 10° for the extreme values of gain shown. In fact, it is NOT a sinusoid. In such a two-cycle sinusoid the maximum value would be at exactly 45° (northeast) off the main axis. In this function, the maximum is lower or higher, depending on the value of g.

Manipulation of (A5) shows the DIFAR bearing of the maximum is

$$b_{d\,\max} = \arcsin\left(\frac{1}{\sqrt{1+g}}\right). \tag{A6}$$

This is graphed in Fig. 17.

Note that this is just the principal bearing value. There will be similar maxima and minima near the corresponding points on the (almost) sine wave; a positive peak at 180° plus $b_{d\,\max}$, and negative peaks at minus $b_{d\,\max}$ and 180 minus $b_{d\,\max}$. The magnitude of the error at that maximum is

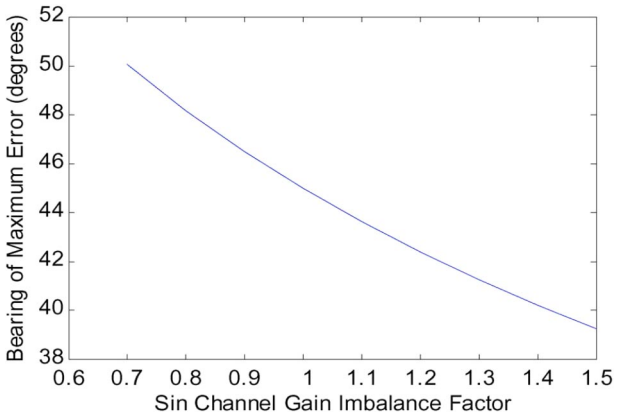

FIG. 17. Bearing of maximum bearing error versus gain imbalance.

$$b_{\text{err max}} = \arctan\left(0.5\left(\sqrt{g} - \frac{1}{\sqrt{g}} \right) \right), \tag{A7}$$

This is plotted in Fig. 18, which presents the magnitude of the maxima and minima of the near-sinusoidal waves.

3. Measuring the actual error and gain factor

The relations above give a feeling for the error behavior as a function of possible gain factors, and the errors observed in Fig. 15 are in the same range. The actual data include random errors from other sources, so we must use a statistical approach to characterize the actual errors while measuring the reference bearing. We do so by fitting a curve similar to Fig. 17 to the distribution in Fig. 16.

The basic equation we use is

$$b_{\text{true}} = b_{\text{ref}} + b_{\text{meas}} - b_{\text{err}}, \tag{A8}$$

where, to review,

b_{true} is the actual true bearing determined by GPS coordinates of the sound projector and the DASAR

b_{ref} is the true bearing of the reference (cosine) channel axis

b_{meas} is the measured bearing of the target from the reference axis

$b_{\text{meas}} = b_d + b_{\text{err}}$

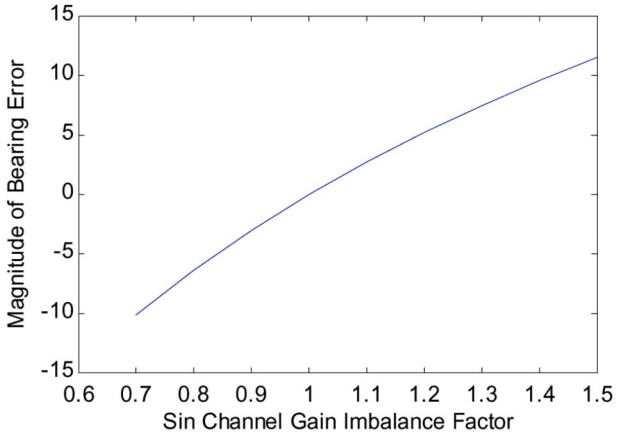

FIG. 18. Maximum magnitude of bearing error versus gain imbalance.

b_d bearing of sound source relative to DASAR reference

b_{err} is the small error due to gain imbalance

We assume b_{err} can be calculated as

$$\begin{aligned} b_{\text{errcalc}} &= a \cdot f(g, b_d) \\ &= a \cdot (\arctan(g \cdot \sin(b_d), \cos(b_d)) - b_d), \end{aligned} \tag{A9}$$

where a is an unknown amplitude and f is a function giving the shape of the error as shown in Fig. 17. The maximum value of this will be $a \cdot f_{\max}$, where $f_{\max}$ is given by Eq. (A7).

We also have a body of measurements allowing us to measure the error for a single trial. From Eq. (A8) we can say

$$b_{\text{errmeas}} = b_{\text{ref}} + b_{\text{meas}} - b_{\text{true}}. \tag{A10}$$

We wish to compare the calculated form and the measured data, and solve for the values of b_{ref} and gain factor g. We do this by a least-squares fit of the function f to the measured data, then solving for the gain and b_{ref}. Because of the nonlinearity of the equations, it is necessary to use a starting guess for g (for instance 1.2), then solve iteratively for new values.

We start with the ith measurement giving $b_{\text{true}}(i)$ and $b_{\text{meas}}(i)$. We assume a starting value for g and calculate $b_d(i)$ as

$$b_d(i) = \arctan(\sin(b_{\text{meas}}(i))/g, \cos(b_{\text{meas}}(i))). \tag{A11}$$

This can be inserted into Eq. (A9) to give a calculated value of the error $b_{\text{calc}}(i)$. The difference of these is the measurement error:

$$\begin{aligned} \text{error}(i) &= b_{\text{errmeas}}(i) - b_{\text{eercalc}}(i) \\ &= b_{\text{ref}}(i) + b_{\text{meas}}(i) - b_{\text{true}}(i) - a^* f(g, b_d(i)). \end{aligned} \tag{A12}$$

One measure of the goodness of a fit is the sum of the squares of all measurements:

$$S = \sum_i \text{error}(i)^2. \tag{A13}$$

We wish to select the parameters b_{ref} and a such that S is a minimum. There will be two simultaneous equations. One is

$$\frac{\partial S}{\partial b_{\text{ref}}} = \sum 2\text{error}(i) \frac{\partial \text{error}(i)}{\partial b_{\text{ref}}} = 0. \tag{A14}$$

Observing from (A12) that

$$\frac{\partial \text{error}(i)}{\partial b_{\text{ref}}} = 1, \tag{A15}$$

Eq. (A14) may be manipulated to the form

$$b^*_{\text{ref}} \sum_i 1 - a^* \sum_i f(i) = \sum_i [b_{\text{true}}(i) - b_{\text{meas}}(i)]. \tag{A16}$$

The second of the two equations is

$$\frac{\partial S}{\partial a} = \sum_i 2\text{error}(i) \frac{\partial \text{error}(i)}{\partial a} = 0. \tag{A17}$$

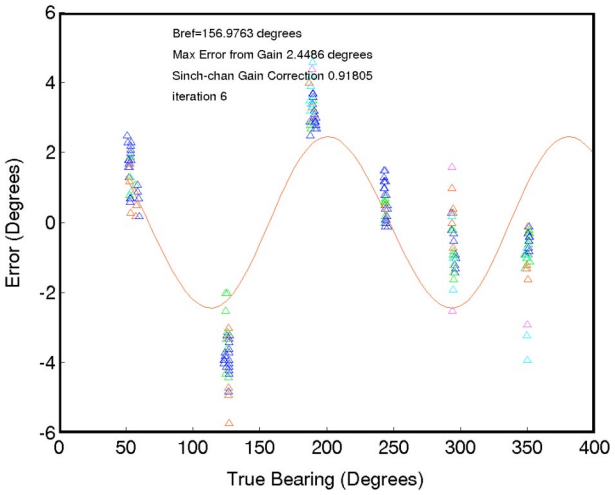

FIG. 19. Measured and computed errors for the ping calibrations for DASAR CBa.

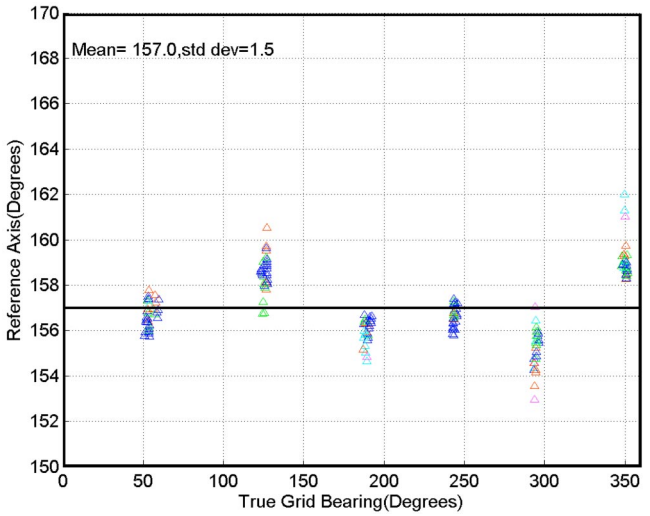

FIG. 20. Reference bearing measurements for DASAR CBa after correcting for gain imbalance.

From (A12)

$$\frac{\partial \text{error}(i)}{\partial a} = -f(i). \tag{A18}$$

Thus Eq. (A17) may be manipulated to give

$$b_{\text{ref}} \sum_i f(i) - a \cdot \sum_i f^2(i) = \sum_i f(i) \cdot (b_{true}(i) - b_{meas}(i)). \tag{A19}$$

Equations (A16) and (A19) are two linear equations for the unknowns b_{ref} and a. In matrix form they are

$$\begin{bmatrix} nm & -\sum f \\ \sum f & -\sum f^2 \end{bmatrix} \begin{bmatrix} b_{\text{ref}} \\ a \end{bmatrix} = \begin{bmatrix} \sum (b_{true} - b_{meas}) \\ \sum f \cdot (b_{true} - b_{meas}) \end{bmatrix}, \tag{A20}$$

where nm is the total number of measurements and all summations are over all measurements. This system can then be solved for b_{ref} and a. b_{ref} is used as is. The value of a is used to improve the estimate of the gain factor as follows: the maximum value of the calculated error is found as $a \cdot f_{\max}$ where $f_{\max}$ is found from Equation (A7) using the old value of g. Then a new value of a is computed by inverting (A7):

$$tbe = \tan(a \cdot f_{\max}), \tag{A21}$$

$$r_g = tbe \pm \sqrt{1 + tbe^2}, \tag{A22}$$

$$g = r_g^2, \tag{A23}$$

where tbe and r_g are just intermediate variables for computing g. Equation (A22) gives two possible values of g that are inverse to each other. If tbe is greater than zero, use the smaller value; if tbe is negative, use the larger.

The entire calculation is then iterated from Eq. (A11) until a approaches a value of 1.000. This implies that g has attained its final value. In typical cases this took around five iterations.

4. Results

Figure 19 shows the measured and calculated values from one such set of measurements. It appears that a substantial proportion of the deviations in Fig. 19 is due to some mechanism such as the gain imbalance. However, there are also other measurement errors.

Once the gain correction factor and reference bearing have been determined for a given DASAR, the correction may be applied in either of two ways:

(1) by calculating the correction factor in degrees for each measurement or
(2) by multiplying the digitized output of the sine channel by the inverse of g before measuring bearings.

The first of these methods is used if the digitized time series has already been used to calculate bearings. The correction is applied to the calculated bearings. The second method is applied if the digitized time series is available but has not already been used for the bearing measurement.

The data plotted in Fig. 15 were processed according to the previous section. b_{ref} was measured as 156.97° with $g = 1.0883$. The error (the difference between measured and true bearings) when plotted against true bearing was (approximately) two cycles of a sine wave with amplitude 2.45°. The data were remeasured after dividing the sine channel by g. The results are in Fig. 20.

The gain imbalance correction reduced the scatter for DASAR CBa from 2.3° to 1.3°. This second data set measured with gain correction was run through the same analysis. The results showed that there was no remaining two-cycle sine wave contribution. Out of curiosity, the data were run again looking for three- and four-cycle sine waves. This showed peak errors of −0.88° and +0.18°, respectively. However, we are not aware of any physical explanation for the apparent three-cycle dependence.

APPENDIX B: LOCALIZATION ACCURACY

The precision of whale call locations, in the form of error (or, more accurately, ''confidence'') ellipses, was esti-

mated following the methods of Lenth (1981) under which individual bearings from a DASAR to a received whale call were assumed to follow a Von Mises distribution (Mardia, 1972). The Von Mises distribution is analogous to the normal distribution, but applies to directional data in which angles x and $x+360°$ are the same. The Von Mises distribution has probability density function

$$f(\theta;\mu,\kappa)=[2\pi I_0(\kappa)]^{-1}\exp[\kappa\cos(\theta-\mu)],$$

where μ is the mean bearing, κ is the concentration parameter, and I_0 is a modified Bessel function. Assuming s is the standard deviation of bearings calculated in the usual way from a random sample of bearings, the concentration parameter can be calculated approximately as

$$\hat{\kappa}^{-1}\approx 2(1-A)+\frac{(1-A)^2(0.48794-0.82905A-1.3915A^2)}{A},$$

$$A=\exp\left[\frac{-1}{2}\left(\frac{s\pi}{180}\right)^2\right].$$

Estimates of s for each DASAR were computed from the gain-corrected calibration data (presented in Sec. III).

Histograms of the differences between gain-corrected bearings and true bearings (known during calibration) confirmed that it was reasonable to assume bearings followed a Von Mises distribution.

When two or more DASARs received the same call, the (x,y) location with maximum statistical likelihood, according to the Von Mises distribution, was used as the estimate of the call's location. Random errors in bearings (observed bearing—true bearing) from each DASAR to a given call were assumed to be independent. The statistical likelihood of the bearings was constructed and maximized as described in footnote 1. An estimate of the variance-covariance matrix of (x,y),

$$Q=\begin{bmatrix}\mathrm{Var}(x) & \mathrm{Cov}(x,y)\\ \mathrm{Cov}(x,y) & \mathrm{Var}(y)\end{bmatrix},$$

was obtained using formulas given in Lenth (1981) and White and Garrott (1990). Relying on the fact that maximum likelihood estimates are asymptotically normally distributed, the area of a 90% confidence ellipse for the true call position was calculated as

$$a=\pi|Q|^{1/2}\cdot\chi^2_{2,0.10},$$

where $\chi^2_{2,0.10}$ was the 10th quantile of a Chi-square distribution having 2 degrees of freedom and $|Q|=\mathrm{Var}(x)\mathrm{Var}(y)-\mathrm{Cov}(x,y)^2$ (White and Garrott, 1990). The length of the major axis of the error ellipse was calculated as

$$l_1=2(\lambda_1\chi^2_{2,0.10})^{1/2},$$

where λ_1 was the largest eigenvalue of Q. Similarly, the angle of the major axis was obtained from the eigenvector corresponding to the largest eigenvalue as

$$\phi_1=\tan^{-1}\left(\frac{\nu_{1,2}}{\nu_{1,1}}\right),$$

where $\nu_{1,1}$ was the first element of the first eigenvector of Q (Mardia *et al.*, 1979).

Not all calls received by 2+ DASARs were localizable or suitable for inclusion in subsequent analyses. Calls were discarded for one of three reasons. (1) A location could not always be computed because the maximum likelihood procedure occasionally failed to converge on a maximum. Generally, this happened when the geometry of the estimated bearings was unfavorable, i.e., when bearings did not intersect, or when multiple bearings intersected at widely separated locations. Convergence failure meant that neither the location nor its covariance could be calculated. (2) In some cases, the maximum likelihood procedure converged on a location estimate, but the variance-covariance matrix, Q, was not positive definite. Positive definite variance-covariance matrices were required for the corresponding error ellipse to have positive area. Nonpositive definite Q tended to occur when bearings were nearly parallel. This typically occurred at locations far from the DASAR array or near lines connecting pairs of DASARs. (3) In a few cases, the maximum likelihood solution was ''behind'' one of the DASARs. This occurred if the angle reported by the DASAR and the angle to the estimated location differed by 180°. For example, if a DASAR reported a bearing to a call of 45°, and the maximum likelihood procedure converged on a location 225° from the DASAR, the solution was ''behind'' the DASAR and was discarded. This situation generally occurred when only two bearings were available and when those two bearings were divergent and did not intersect (except if one or both bearings were changed by 180°).

To map the typical precision of the estimated call locations near the DASAR array, values of a (error ellipse size), l_1 (long axis length), and ϕ_1 (angle of long axis) were calculated for each call and smoothed using a kernel density estimator modified for continuous data. The usual Gaussian kernel density estimator for point location data (Wand and Jones, 1995) was modified for continuous data by multiplying values of the continuous variable by the usual kernel weights and computing a weighted average, i.e.,

$$\hat{\mu}(y|x)=\frac{\Sigma_{i=1}^n w(x,X_i,h)y_i}{\Sigma_{i=1}^n w(x,X_i,h)},$$

where $\hat{\mu}(y|x)$ was the estimated mean of variable y at location x (e.g., $y=$ area of 90% confidence ellipse), X_i was the coordinates of the ith observed location, y_i was the value of the continuous variable at the ith observed location, h was the smoothing parameter, and

$$w(x,X_i,h)=\exp\left[\frac{1}{2h^2}(x-X_i)^T(x-X_i)\right]$$

(Bailey and Gatrell, 1995). The smoothing parameter h dictated the degree of smoothing and for this analysis h was set to 1000 m. The weighted average, $\hat{\mu}(y|x)$, was computed at every intersection of a 500×500 m grid. The resulting surface of $\hat{\mu}(y|x)$ was then plotted for inspection.

[1]The statistical likelihood was a function of the unknown parameters κ and μ_i, where $i=1,2,...$ indexed the various DASARs receiving the call. The statistical likelihood represented the probability of observing the entire set

of bearings given hypothetical values of μ_i and κ. To assure that all μ_i intersected at a common point, the statistical likelihood was reparametrized by setting $\mu_i = \arctan((y-y_i)/(x-x_i))$, where (x_i, y_i) was the location of the ith DASAR and (x,y) was the point where all μ_i intersected. After reparametrization, the statistical likelihood was a function of the unknown parameters x, y, and κ. Given estimates of κ from the calibration data, estimates of x and y (the call's location) were obtained by repeatedly evaluating the statistical likelihood over a range of values until the probability of the observed bearings was maximized. The (x,y) point that maximized the statistical likelihood was used as the estimate of the call's location.

Bailey, T. C., and Gatrell, A. C. (**1995**). *Interactive Spatial Data Analysis* (Longman Scientific & Technical, Essex, UK).

Blackwell, S. B., and Greene, Jr., C. R. (**2004**). ''Sounds from an oil production island in the Beaufort Sea in summer: characteristics and contribution of vessels,'' to be submitted to J. Acoust. Soc. Am. Available from Greeneridge Sciences, 1411 Firestone Road, Goleta, CA 93117; info@greeneridge.com.

Clark, C. W., and Ellison, W. T. (**2000**). ''Calibration and comparison of the acoustic location methods used during the spring migration of the bowhead whale, *Balaena mysticetus*, off Pt. Barrow, Alaska, 1984–1993,'' J. Acoust. Soc. Am. **107**, 3509–3517.

Clark, C. W., and Johnson, J. H. (**1984**). ''The sounds of the bowhead whale, *Balaena mysticetus*, during the spring migrations of 1979 and 1980,'' Can. J. Zool. **62**(7), 1436–1441.

Clark, C. W., Charif, R., Mitchell, S., and Colby, J. (**1996**). ''Distribution and behavior of the bowhead whale, *Balaena mysticetus*, based on analysis of acoustic data collected during the 1993 spring migration off Point Barrow, Alaska,'' Rep. Int. Whal. Comm. **46**, 541–552.

Greene, C. R. (**1987**). ''Acoustic studies of underwater noise and localization of whale calls,'' Chap. 2, in ''Responses of bowhead whales to an offshore drilling operation in the Alaskan Beaufort Sea, autumn 1986,'' Report from LGL Ltd., King City, Ontario, and Greeneridge Sciences Inc., Santa Barbara, CA, for Shell Western E & P Inc., Anchorage, AK. Available from Greeneridge Sciences, 1411 Firestone Road, Goleta, CA; info@greeneridge.com.

Greene, C. R., Jr., McLennan, M. W., McDonald, T. L., and Richardson, W. J. (**2002**). ''Acoustic monitoring of bowhead whale migration, autumn 2001,'' in ''Monitoring of industrial sounds, seals, and whale calls during construction of BP's Northstar oil development, Alaskan Beaufort Sea, 2001, Draft, October 2002 ed.,'' edited by W. J. Richardson and M. T. Williams. LGL Rep. TA2573-2. Report from LGL Ltd., King City, Ontario, and Greeneridge Sciences Inc., Santa Barbara, CA, for BP Exploration (Alaska) Inc., Anchorage, AK, and Nat. Mar. Fish. Serv., Anchorage, AK, and Silver Spring, MD. pp. 8-1 to 8–79. Available from Greeneridge Sciences, Inc., 1411 Firestone Road, Goleta, CA 93117; info@greeneridge.com

Lenth, R. V. (**1981**). ''On finding the source of a signal,'' Technometrics **23**, 149–154.

Ljungblad, D. K. (**1986**). ''Endangered whale aerial surveys in the Navarin Basin and St. Matthew Hall planning areas, Alaska,'' in ''Aerial surveys of endangered whales in the northern Bering, eastern Chukchi, and Alaskan Beaufort Seas, 1985: with a seven year review, 1979–85,'' Appendix E in NOSC Tech. Rep. 1111; OCS Study MMS 86-0002. Report from Naval Ocean Systems Center, San Diego, CA, for U.S. Minerals Manage. Serv., Anchorage, AK. NTIS AD-A172 753/6.

Mardia, K. V. (**1972**). *Statistics of Direction Data* (Academic, New York).

Mardia, K. V., Kent, J. T., and Bibby, J. M. (**1979**). *Multivariate Analysis* (Academic, London).

McDonald, T. L., and Richardson, W. J. (**2003**). ''A statistical approach for assessing displacement of bowhead whale locations associated with elevated sound levels,'' LGL Rep. TA2706-4. Chap. 9, in ''Monitoring of industrial sounds, seals, and bowhead whales near BP's Northstar oil development, Alaskan Beaufort Sea, 1999–2002,'' edited by W. J. Richardson and M. T. Williams. Report from LGL Ltd., King City, Ontario, and Greeneridge Sciences Inc., Santa Barbara, CA, for BP Exploration (Alaska) Inc., Anchorage, AK, and Nat. Mar. Fish. Serv., Anchorage, AK, and Silver Spring, MD. pp 9–1 to 9–26. Available from Greeneridge Sciences Inc., 1411 Firestond Road, Goleta, CA 93117; info@greeneridge.com.

McLennan, M. W., and Greene, C. R., Jr. (**1996**). ''Passive acoustic localization and tracking of vocalizing marine mammals using buoy and line arrays,'' Appendix in ''Report of the cetacean acoustic assessment workshop,'' report by Australian Nature Conservation Agency (now Biodiversity Group of Environment Australia), Hobart, Tas.

Mellinger, D. K., and Clark, C. W. (**1997**). ''Methods for automatic detection of mysticete sounds.'' Mar. Freshwater Behav. Physiol. **29**(1–4), 163–181.

Mellinger, D. K., and Clark, C. W. (**2000**). ''Recognizing transient low-frequency whale sounds by spectrogram correlation,'' J. Acoust. Soc. Am. **107**, 3518–3529.

Moore, S. E., and Reeves, R. R. (**1993**). ''Distribution and movement,'' in *The Bowhead Whale*, edited by J. J. Burns, J. J. Montague, and C. J. Cowles. (Spec. Publ. 2. Soc. Mar. Mammal., Lawrence, KS), pp. 313–386.

Richardson, W. J., Miller, G. W., and Greene, Jr., C. R. (**1999**). ''Displacement of migrating bowhead whales by sounds from seismic surveys in shallow waters of the Beaufort Sea,'' J. Acoust. Soc. Am. **106**(4 Pt 2), 2281(A).

Richardson, W. J., Greene, C. R., Jr., Malme, C. I., and Thomson, D. H. (**1995**). *Marine Mammals and Noise* (Academic, San Diego).

Stoker, S. W., and Krupnik, I. I. (**1993**). ''Subsistence whaling,'' in *The Bowhead Whale* edited by J. J. Burns, J. J. Montague, and C. J. Cowles (Spec. Publ. 2, Soc. Mar. Mammal., Lawrence, KS), pp. 579–629.

Swartz, S. L., Cole, T., McDonald, M. A., Hildebrand, J. A., Oleson, E. M., Martinez, A., Clapham, P. J., Barlow, J., and Jones, M. L. (**2003**). ''Acoustic and visual survey of humpback whale (*Megaptera novaeangliae*) distribution in the eastern and southern Caribbean Sea,'' Carib. J. Sci. **39**, 195–208.

Wand, M. P., and Jones, M. D. (**1995**). *Kernel Smoothing* (Chapman & Hall/CRC, Boca Raton, FL).

White, G. C., and Garrott, R. A. (**1990**). *Analysis of Wildlife Radio-tracking Data* (Academic, New York).

Würsig, B., and Clark, C. (**1993**). ''Behavior,'' in *The Bowhead Whale*, edited by J. J. Burns, J. J. Montague, and C. J. Cowles (Spec. Publ. 2. Soc. Mar. Mammal., Lawrence, KS), pp. 157–199.